

Experiments in Rainfall Estimation with a Polarimetric Radar in a Subtropical Environment

EDWARD A. BRANDES, GUIFU ZHANG, AND J. VIVEKANANDAN

National Center for Atmospheric Research, Boulder, Colorado*

(Manuscript received 20 July 2001, in final form 24 January 2002)

ABSTRACT

A unique dataset consisting of high-resolution polarimetric radar measurements and dense rain gauge and disdrometer observations collected in east-central Florida during the summer of 1998 was examined. Comparison of the radar measurements and radar parameters computed from the disdrometer observations supported previous studies, which indicate that oscillating drops in the free atmosphere have more spherical apparent shapes in the mean than equilibrium shapes. Radar–disdrometer comparisons improved markedly when using an empirical axis ratio relation developed from observational studies and representing more spherical drop shapes. Fixed-form power-law rainfall estimators for radar reflectivity (Z_H), specific differential phase (K_{DP}), specific differential phase–differential reflectivity (K_{DP} , Z_{DR}), and radar reflectivity–differential reflectivity (Z_H , Z_{DR}) were then determined using the disdrometer observations. Relations were produced for both equilibrium shapes and the empirical axis ratios. Polarimetric rainfall estimators based on more spherical shapes gave significantly improved performance. However, the improvement was largely in bias mitigation. Rainfall estimates with the Z_H – Z_{DR} measurement pair had the highest correlation with rain gauge observations, the smallest range in bias factors from storm to storm, and the smallest root-mean-square error.

1. Introduction

Recent research indicates that polarimetric measurements (differential propagation phase and differential reflectivity) can improve radar estimates of rainfall. Estimates derived from specific differential phase (K_{DP}), defined as one-half the range derivative of the two-way differential propagation phase (Φ_{DP}), are not susceptible to hardware calibration error and attenuation and are relatively unaffected by beam blockage and anomalous propagation (Ryzhkov and Zrnić 1995a,b; Zrnić and Ryzhkov 1996; Ryzhkov et al. 1997; Vivekanandan et al. 1999; Brandes et al. 2001). Sachidananda and Zrnić (1987) determined that the relation between K_{DP} and rainfall rate is fairly linear and that K_{DP} is insensitive to drop size distribution (DSD) variations. The parameter is also insensitive to the presence of dry, tumbling hail (Balakrishnan and Zrnić 1990; Aydin et al. 1995). A few potential problems have been identified. Sidelobe contamination can cause bias in estimates of K_{DP} (Sachidananda and Zrnić 1987). Negative K_{DP} values may arise from statistical fluctuations in Φ_{DP} , precipitation

gradients (Ryzhkov and Zrnić 1996, 1998; Brandes et al. 2001), and the presence of Mie scatterers (e.g., Smyth et al. 1999). Rainfall tends to be underestimated when drops are small (Ryzhkov and Zrnić 1996; Brandes et al. 2001). Because differential propagation measurements have accuracies of a few degrees, they are filtered in range prior to the computation of K_{DP} . Bias is introduced by inhomogeneities within the filtering interval (Sachidananda and Zrnić 1987; Gorgucci et al. 1999, 2000).

The differential reflectivity (Z_{DR}), defined as the ratio of radar reflectivities at horizontal and vertical polarization (Seliga and Bringi 1976), is sensitive to the flattening of raindrops and increases with drop size. Rainfall estimates made with the radar reflectivity (Z_H) and differential reflectivity measurement pair respond to size variations and have smaller errors than estimates determined from radar reflectivity alone (Seliga and Bringi 1976; Ulbrich and Atlas 1984). This benefit extends to rainfall estimators that combine K_{DP} and Z_{DR} (Jameson 1991; Ryzhkov and Zrnić 1995a). Chandrasekar et al. (1990) assert that random error in Z_{DR} measurements dictate that the improvement with differential reflectivity-based estimators is at moderate to heavy rain rates. Hail is associated with low differential reflectivity, because hail generally tumbles as it falls. Rain rates derived with hail-contaminated measurements can become very large. Mismatches in radar beam patterns at horizontal and vertical polarization and sidelobes are sour-

* The National Center for Atmospheric Research is sponsored by the National Science Foundation.

Corresponding author address: Dr. Edward A. Brandes, National Center for Atmospheric Research, P.O. Box 3000, Boulder, CO 80307.
E-mail: brandes@ncar.ucar.edu

es of bias in Z_{DR} measurements (e.g., Herzegh and Jameson 1992) and, hence, in rainfall estimates.

Simulations and studies with drop-size observations (Ulbrich and Atlas 1984; Seliga et al. 1986; Sachidananda and Zrnić 1987; Jameson 1991; Aydin and Giridar 1992; Ryzhkov and Zrnić 1995a) suggest that error reductions with polarimetric rainfall estimators (using radar reflectivity-based rainfall estimates as a benchmark) should be a factor of 2 or more depending on the rain rate. Rainfall estimates made with polarimetric radar measurements, on the other hand, have shown small to moderate improvements. Seliga et al. (1981) found that an estimator based on reflectivity and differential reflectivity had a fractional standard error (FSE) of 16% as compared with 19% for radar reflectivity. Ryzhkov and Zrnić (1995a) found errors averaged 28% with the specific differential phase parameter and 38% with an estimator based on a combination of reflectivity and differential reflectivity. Errors with the specific differential phase and differential reflectivity measurement pair were 19%–22%. By comparison, the error with radar reflectivity was 31%. Gorgucci et al. (1995) determined errors of 49%–58% for reflectivity and 35% for the reflectivity–differential reflectivity combination. Ryzhkov and Zrnić (1996) found marked improvement with K_{DP} ; errors were 14% as compared with 38% with radar reflectivity. Brandes et al. (2001) found that reflectivity and specific differential phase estimators, after removing a storm with small drops, were essentially equivalent. The smaller error reduction in these observational studies probably comes from factors other than random measurement error, such as sampling issues, sidelobe problems, mismatches between the horizontal and vertical beams of the radar, and loss of polarimetric purity.

Polarimetric radar measurements are sensitive to hydrometeor size, shape, orientation, and composition. Rainfall rates derived from them are influenced by the mean drop shape and by drop canting. There has been much effort to determine the shape of falling raindrops. [See Keenan et al. (2001) for a review of the observational data, empirical axis-ratio relations derived from them, and relations based on theoretical considerations.] Pruppacher and Beard (1970), Green (1975), and Beard and Chuang (1987) examined “equilibrium” shapes, that is, the mean shape of drops falling under the influence of gravity and subject to a balance of forces acting at the water–air interface. Other studies revealed the importance of vortex shedding, collisions, and turbulence or wind shear (Pruppacher and Pitter 1971; Beard and Jameson 1983; Beard et al. 1983; Beard and Kubesh 1991), which cause drops in the free atmosphere to oscillate with axisymmetric and transverse modes and to have mean shapes that differ from equilibrium. The oscillations result in an apparent or effective radar shape as defined by backscattered returns (typically at horizontal and vertical polarization).

Goddard et al. (1982) compared Z_{DR} values computed

from disdrometer observations, using the equilibrium shapes of Pruppacher and Beard (1970), with radar measurements and found that disdrometer-based Z_{DR} values exceeded radar measurements by 0.3 dB on average. They reasoned that the radar-observed drops were more spherical than the equilibrium shapes assumed in the disdrometer calculations. Goddard and Cherry (1984) compared radar measurements with disdrometer calculations using the axis ratios of Pruppacher and Pitter (1971) and found that the disdrometer estimates of Z_{DR} were 0.1 dB higher than the radar estimates. The argument for more spherical mean shapes is also supported by drop observations made by aircraft (Chandrasekar et al. 1988; Bringi et al. 1998) and by recent laboratory experiments (Andsager et al. 1999) that indicate Z_{DR} values computed from observed oscillating drops are 0.1–0.4 dB less than those determined from equilibrium axis ratios. Sachidananda and Zrnić (1987) conducted an experiment in which the axis ratios were allowed to vary and found that K_{DP} rain rates changed by 18%. Chandrasekar et al. (1990) found K_{DP} rain-rate differences of 30% to 50% for estimators based on experimentally determined and equilibrium axis ratios.

The goal of this study is to further clarify the utility of polarimetric measurements for estimating rainfall. Radar parameters computed from disdrometer observations and rain gauge observations serve as comparative standards. We begin with a description of the radar data, rain gauge observations, and disdrometer observations available for study. Fixed-form polarimetric rainfall estimators, that is, relationships with constant coefficients and exponents, are examined to determine axis ratio impacts on estimated rainfalls. Our earlier efforts with $\mathfrak{R}(Z_H)$ and $\mathfrak{R}(K_{DP})$ rain-rate estimators (Brandes et al. 2001) are extended to the evaluation of $\mathfrak{R}(K_{DP}, Z_{DR})$ and $\mathfrak{R}(Z_H, Z_{DR})$ estimators.

2. Data

During the summer of 1998 the National Center for Atmospheric Research’s S-band, dual-polarization radar (S-Pol) was deployed in east-central Florida during a special field experiment (PRECIP98) to evaluate the potential of polarimetric radar to estimate rainfall in a subtropical environment. The experiment coincided with a field component of the National Aeronautics and Space Administration’s Tropical Rainfall Measuring Mission dubbed the Texas and Florida Underflights Experiment (TEFLUN-B).

S-Pol was placed 26 km south-southwest of the operational Weather Surveillance Radar-1988 Doppler (WSR-88D) at Melbourne, Florida, (KMLB; Fig. 1). S-Pol characteristics relevant to this study are described by Brandes et al. (2001). The radar operated daily from 21 July until 28 September 1998. Emphasis was on rainfall estimation. In this study we compare estimates derived from polarimetric variables with rainfall observations obtained from a dense rain gauge network at the

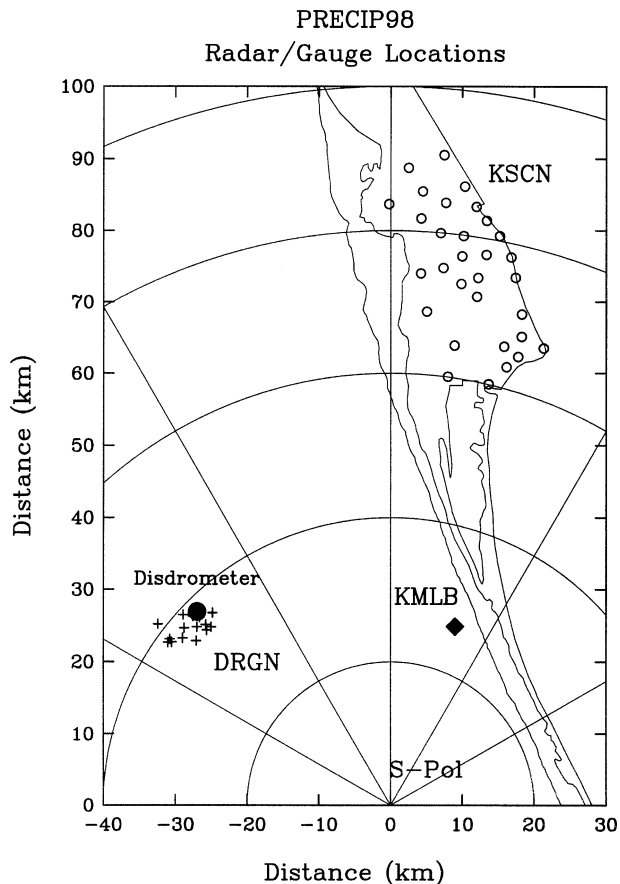


FIG. 1. Location of rain gauges within DRGN and KSCN. Also shown are the locations of KMLB and NCAR's S-Pol radar. The DRGN disdrometer site is denoted with a large solid circle. Coordinates are from S-Pol.

Kennedy Space Center (KSCN) and from a special network with gauges installed singly and in small clusters (DRGN; Fig. 1). The KSCN was 60–90 km from the radar and the DRGN was 35–41 km. Both networks consisted of tipping-bucket gauges that recorded either the clock time of each tip or the number of tips in 10-s intervals. Each tip corresponded to 0.01 in. (0.254 mm) of rainfall. Tipping-bucket gauges tend to underestimate rainfall as the wind speed and precipitation intensity increase (Sevruk 1996). Instrumentation within the DRGN included a video disdrometer (Schönhuber et al. 1997; Nešpor et al. 2000).

The selection of statistical parameters for comparing radar-rainfall estimates and gauge observations is not trivial. Parameters chosen here are the bias factor (computed as the sum of the observations at gauges reporting rainfall divided by the sum of the radar estimates at those gauges, or $\sum G/\sum R$), the correlation coefficient between gauge-observed and radar-estimated rainfall accumulations, the root-mean-square error (rmse) of the radar estimates, and the rmse after removing estimator bias. Each parameter has particular strengths and weaknesses, but the ensemble provides a simple basis for

comparison and facilitates comparison with previous studies.

The DRGN (Fig. 1) is not ideal for evaluating radar-rainfall estimates. The network is relatively small in size when compared with rain swaths from Florida convective storms, the number of gauges is small, and the gauge density is not uniform. Statistics can be dominated by a single cluster of gauges or by a single stage of storm development. Strong rainfall gradients often associate with extremely high correlation coefficients between radar-rainfall estimates and gauge observations; weak gradients can cause very low correlation coefficients even though rmse are small. Generally, computed parameters varied more broadly within the DRGN than the KSCN. Mean bias factors for the two networks differed slightly (section 3b).

a. Radar

Standard radar calibration procedures include the input of test pulses to establish receiver noise level and system gains. Radar reflectivity and differential reflectivity measurements are corrected for attenuation with the differential propagation phase measurement using empirical relations similar to those described by Ryzhkov and Zrníć (1994). Measurement errors are thought to be 1 dB for radar reflectivity and <0.2 dB for differential reflectivity. System calibration is verified by making consistency checks among radar reflectivity, differential reflectivity, and specific differential phase (Goddard et al. 1994; Scarchilli et al. 1996). Comparisons on three days indicated that radar reflectivity was 0.45–0.85 dB too low. Consequently, the average difference (0.65 dB) was added to the reflectivity measurements. Calibration procedures include the collection of vertically pointing data whenever light to moderate rainfall occurs at the radar site. Effects of preferred particle orientations should be absent at vertical incidence and the differential reflectivity should be close to 0 dB. Such checks typically disclose Z_{DR} biases of $<\pm 0.05$ dB.

The specific differential phase is the range derivative of the measured differential propagation phase. Because the basic measurement has a large standard error (3° – 4°), Φ_{DP} is filtered in range. The algorithm used to compute K_{DP} , described by Ryzhkov and Zrníć (1996), produces lightly and heavily filtered versions of K_{DP} by smoothing over 17 data bins (2.4 km) and 49 data bins (7.2 km), respectively. Ryzhkov and Zrníć estimate errors are 0.04° – $0.10^\circ \text{ km}^{-1}$ for the heavily filtered version of K_{DP} and 0.12° – $0.30^\circ \text{ km}^{-1}$ for the lightly filtered version. Aydin et al. (1995) estimate errors in strong convection are close to $0.50^\circ \text{ km}^{-1}$. In previous studies (Ryzhkov and Zrníć 1996; Brandes et al. 2001) the less (more) smoothed version of K_{DP} was used for rainfall estimation if the radar reflectivity was >40 dBZ (≤ 40 dBZ). This procedure often yields higher rainfall estimates than those determined exclusively from either the

lightly or heavily filtered versions of K_{DP} . An implicit assumption is that Φ_{DP} is linear over the distance for which K_{DP} is computed. Filtering introduces bias, which can be positive or negative, whenever the distribution of precipitation is not uniform (Sachidananda and Zrnić 1987; Gorgucci et al. 1999). In an attempt to reduce the bias K_{DP} values were “corrected” following the procedure of Gorgucci et al. (1999). Experience shows that the net effect on accumulated rainfalls is small for an ensemble of gauges. Correlation coefficients between radar-estimated rainfalls and gauge observations generally increase negligibly. In order to minimize filtering bias and to prevent the introduction of bias by selecting from two filtered interpretations of K_{DP} , only adjusted values from the less-filtered version of K_{DP} are used for rainfall estimation in this study. Mean values of the lightly and heavily filtered measures of K_{DP} are identical; rain rates from the lightly filtered K_{DP} values are $\sim 5\%$ higher because of estimator nonlinearities. Correlation coefficients between radar and gauge amounts tend to be slightly lower for the less-filtered K_{DP} .

Routinely the S-Pol radar made 360° scans at 0.5° antenna elevation and at intervals ranging from 55 s to 1 min 50 s. Polarimetric measurements (radar reflectivity, differential reflectivity, differential phase, copolar correlation coefficient, and linear depolarization ratio) were obtained to a range of 175 km. Whenever significant rainfall occurred over the DRGN and KSCN, special datasets with high temporal resolution at low antenna elevation or frequent volumetric samples were collected. For some events, the temporal resolution at low elevation is 20 s or less. The spatial resolution is generally 0.15 km in range and 0.9° in azimuth. Rainfall accumulations were on polar grids of $0.15 \text{ km} \times 1^\circ$ spacing. For validation, radar-derived rainfalls were compared with gauge observations. Factors which influence the results are summarized by Brandes et al. (2001) and described in references therein. Under ideal conditions with a well-calibrated radar and an unbiased rainfall-rate estimator only approximate agreement between radar-derived rainfall estimates and gauge observations is expected.

b. Disdrometer

Disdrometer data for 17 rainfall events were available for study. The information included 1-min drop counts of equivalent-volume diameters (D , mm) quantized in size categories of 0.2 mm. The range in tabulated drop diameters was 0.1–8.1 mm. As with rain gauges, observations are subject to wind-induced errors (Nešpor et al. 2000). Small drops are most affected; counts can be over- or underestimated.

Radar reflectivity, differential reflectivity, and specific differential phase were determined from the observed DSDs and calculated scattering amplitudes using the T-matrix method (Ishimari 1991) as described by

Zhang et al. (2001a). Rain rates (R , mm h^{-1}) were computed from

$$R = 6\pi \times 10^{-4} \int_0^{D_{\max}} D^3 N(D) v_t(D) dD, \quad (1)$$

where D_{\max} is the diameter of the largest observed drop, $N(D)$ is the drop number concentration ($\text{mm}^{-1} \text{m}^{-3}$), and v_t is the drop terminal velocity (m s^{-1}). The velocity was computed from

$$v_t = -0.1021 + 4.932D - 0.9551D^2 + 0.07934D^3 - 0.002362D^4,$$

an expression derived from the laboratory measurements of Gunn and Kinzer (1949) and Pruppacher and Pitter (1971).

c. Radar–disdrometer comparison

Radar reflectivity factor (Z_H), differential reflectivity (Z_{DR}), and specific differential phase (K_{DP}) as determined from radar measurements and computed from disdrometer observations were compared for long-lived events occurring on 8 and 20 August and 17 September. As noted previously, the radar estimates of K_{DP} were computed by filtering Φ_{DP} measurements over a range interval of 17 data bins (2.4 km). Radial distributions of Z_H and Z_{DR} were averaged (linear values) over 5 data bins (0.75 km) to make the radar measurements more compatible with the 1-min disdrometer samples. Some uncertainty is likely when comparing two fundamentally different instruments. The large distance between the radar and the disdrometer (38 km), resulting in huge sampling volume differences and differences in heights of the two measurements (roughly 400 m), weighs heavily on the comparison.

Because of their application in many studies and as a reference for estimator sensitivity to axis ratios, disdrometer calculations were first performed using the equilibrium axis ratios of Green (1975). In the mean, the disdrometer reflectivity values were 0.20 dB higher than that measured by radar (Table 1). Differential reflectivity values averaged 0.25 dB larger than those measured with radar. This difference is much bigger than bias errors found by tilting the radar antenna vertically; hence, the basic radar measurement is not the source of the discrepancy. The difference is within the range of values and similar in sign to the studies of Goddard et al. (1982), Goddard and Cherry (1984), Chandrasekar et al. (1988), and Andsager et al. (1999). As concluded by these investigators, the discrepancy is thought to originate with drop oscillations resulting in mean shapes that are more spherical than the equilibrium values.

An experiment was conducted to determine the impact of different drop shapes on the value of disdrometer-derived Z_{DR} . An axis ratio relation representing more spherical drop shapes was determined by com-

TABLE 1. Comparison of mean radar reflectivity (Z_H), differential reflectivity (Z_{DR}), and specific differential propagation phase (K_{DP}), as determined from radar measurements and computed from disdrometer observations collected on 8 Aug, 21 Aug, and 17 Sep. Equilibrium axis ratios are given by Green (1975). The empirical axis ratios are given by Eq. (2). Disdrometer–radar differences are shown parenthetically. The reflectivity measurements include a +0.65 dB adjustment based on a consistency check among polarimetric variables (see text). Round-off influences some numbers (332 data points).

	Z_H	Z_{DR}	K_{DP}
Radar measurements	32.0 dBZ	0.70 dB	0.15° km ⁻¹
Disdrometer estimates			
Equilibrium axis ratios	32.2 dBZ (0.20 dB)	0.95 dB (0.25 dB)	0.26° km ⁻¹ (0.11° km ⁻¹)
Empirical axis ratios [Eq. (2)]	32.0 dBZ (0.05 dB)	0.76 dB (0.06 dB)	0.21° km ⁻¹ (0.06° km ⁻¹)

binning the observations of Pruppacher and Pitter (1971), Chandrasekar et al. (1988), Beard and Kubesh (1991), and Andsager et al. (1999) to derive

$$r = 0.9951 + 0.025 10D - 0.036 44D^2 + 0.005 030D^3 - 0.000 249 2D^4, \quad (2)$$

where r is the axis ratio (here vertical axis divided by the horizontal axis) and D (mm) is the equivalent-volume drop diameter. This relation yields axis ratios that are significantly more spherical than were found by Pruppacher and Beard (1970) and Green (1975), particularly for drops with $1 \leq D \leq 4$ mm. It agrees quite well with the relationship of Andsager et al. [1999, their Eq. (1)], except for large drops ($D > 5$ mm) where that study differs from the observations of Pruppacher and Pitter (1971). The more spherical shapes reduced the average Z_H difference to 0.05 dB and the average Z_{DR} difference to 0.06 dB. The utility of Eq. (2) is also supported by agreement between accumulated rainfalls from radar and gauges (section 3b).

The mean K_{DP} values are 0.15° km⁻¹ for the radar and 0.26° km⁻¹ for the disdrometer when equilibrium axis ratios are used (Table 1). Such a discrepancy would cause large underestimates of rainfall if the problem lay entirely with the radar. Allowing for more spherical axis ratios reduces the difference to 0.06° km⁻¹. This is a sizable residual difference given that the mean radar estimate is only 0.15° km⁻¹. The remaining discrepancies in Z_{DR} and K_{DP} could be reduced still further by allowing for increased oscillations due to drop collisions (e.g., Beard et al. 1983; Beard 1984), but sampling issues may also contribute to the differences. Regardless, the comparison between radar and disdrometer values of Z_{DR} and K_{DP} is much improved if the empirical (more spherical) axis ratios given by Eq. (2) are used in the calculations.

Radar measurements and disdrometer-derived parameters based on the empirical axis ratios are presented in Fig. 2. While the mean values of radar reflectivity agree quite well (Fig. 2a), at low (high) radar reflectivity radar values exceed (are less than) those of the disdrometer—probably due to the filtering performed and to radar beam-smoothing. For reflectivity >45 dBZ the disdrometer values are about 4 dB higher. The Z_{DR} comparison (Fig. 2b) is also good (cf. Goddard and Cherry 1984).

“Outliers” in the reflectivity and differential reflectivity plots are characterized by data pairs with relatively large radar and small disdrometer values. These data points could be caused by small numbers of large drops at the leading edges of convective storms that are missed by the small sampling volume of the disdrometer. Figure 2c presents a comparison of specific differential phase, as estimated from radar measurements and as calculated from disdrometer observations. It is readily apparent that for large K_{DP} the radar-derived values are considerably smaller than those derived from disdrometer observations. For small K_{DP} , radar values average a little larger than the disdrometer values. The steep slope of the distribution and the absence of outlier points seen in Figs. 2a,b are likely due to the filtering of Φ_{DP} .

3. Experiments with fixed rain-rate relations

a. Computation of estimators

Following Zhang et al. (2001a), Z_H , Z_{DR} , and K_{DP} were calculated for equilibrium axis ratios and for the empirical relation Eq. (2). Power-law estimators were then determined by the least squares method using rain rates computed with Eq. (1) as the dependent variable. The results are

for the Green (1975) equilibrium axis ratios:

$$R = 2.47 \times 10^{-2} Z_H^{0.692} \quad (3)$$

$$R = \text{sign}(K_{DP}) 46.1 |K_{DP}|^{0.873} \quad (4)$$

$$R = \text{sign}(K_{DP}) 88.3 |K_{DP}|^{0.982} Z_{DR}^{-1.89} \quad (5)$$

$$R = 7.86 \times 10^{-3} Z_H^{0.967} Z_{DR}^{-4.98} \quad (6)$$

and for empirical axis ratios:

$$R = 2.62 \times 10^{-2} Z_H^{0.687} \quad (7)$$

$$R = \text{sign}(K_{DP}) 54.3 |K_{DP}|^{0.806} \quad (8)$$

$$R = \text{sign}(K_{DP}) 136 |K_{DP}|^{0.968} Z_{DR}^{-2.86} \quad (9)$$

$$R = 7.46 \times 10^{-3} Z_H^{0.945} Z_{DR}^{-4.76} \quad (10)$$

b. Results

Rainfall estimates were made with all relations [Eqs. (3)–(10)] for 25 events occurring in the two gauge net-

PRECIP98: S-Pol/Disdrometer Comparison

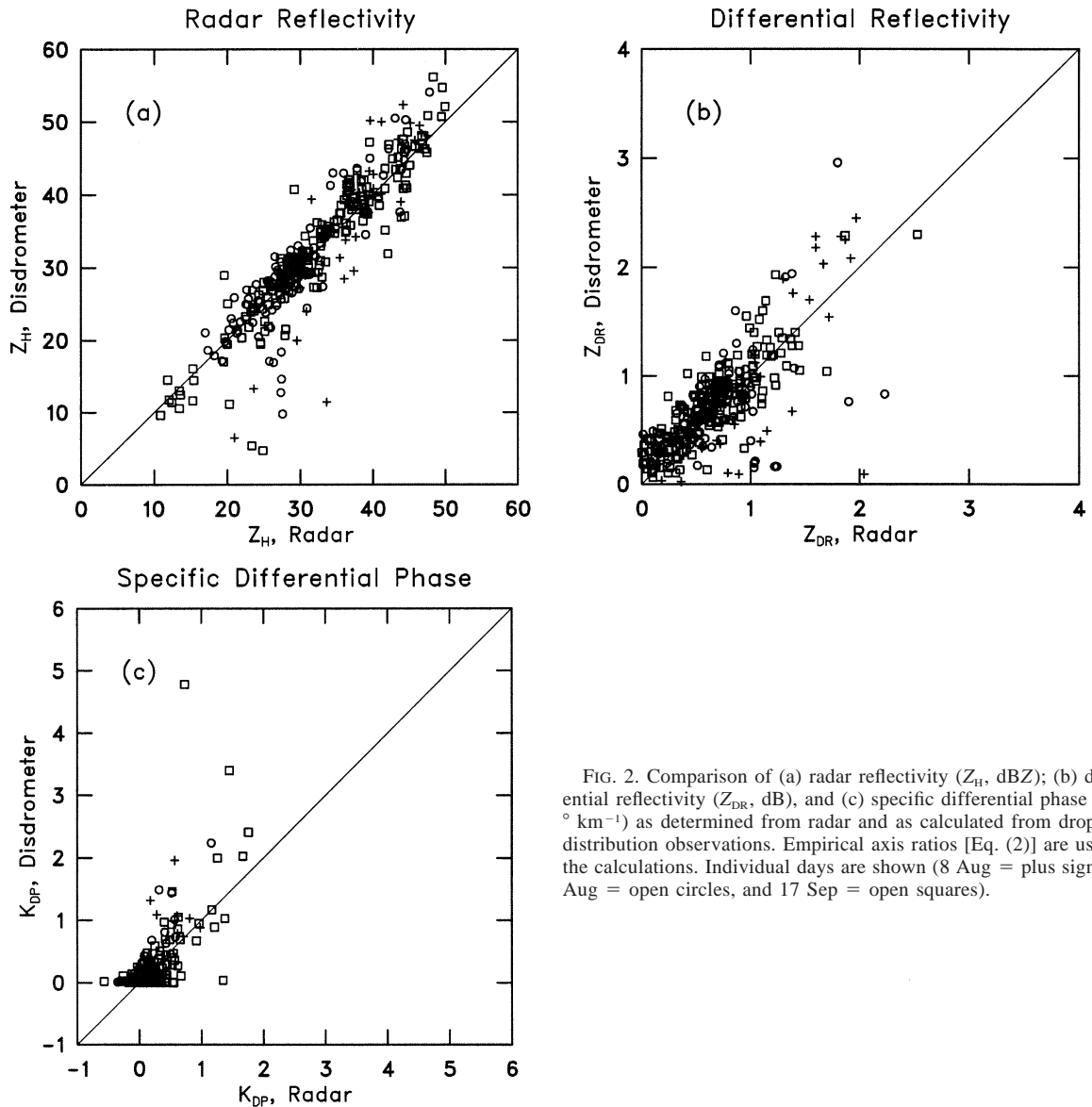


FIG. 2. Comparison of (a) radar reflectivity (Z_H , dBZ); (b) differential reflectivity (Z_{DR} , dB), and (c) specific differential phase (K_{DP} , $^{\circ} \text{ km}^{-1}$) as determined from radar and as calculated from drop size distribution observations. Empirical axis ratios [Eq. (2)] are used in the calculations. Individual days are shown (8 Aug = plus signs, 21 Aug = open circles, and 17 Sep = open squares).

works on 17 storm days. Storm durations were 1–8 h. Summary results for the various estimators are presented in Table 2; results for individual storms with estimators using the empirical axis ratio relation are shown in Table 3. The latter are stratified according to the two gauge networks to indicate spatial and temporal variability. Inspection of Eqs. (3) and (7) and Table 2 reveals that radar reflectivity estimators are insensitive to the assumed drop shape. Overall bias factors, based on 388 radar–gauge comparisons, vary by about 1% and disclose a small rainfall overestimate of $\sim 5\%$. As in numerous studies, bias factors for radar reflectivity vary considerably from storm to storm. Using the results for the $\mathfrak{R}(Z_H)$ estimator based on more spherical shapes (Table 3) as an example, we find that bias factors vary

from 0.62 (a large rainfall overestimate) for the DRGN event on 6 August to 1.56 for the DRGN event on 20 September. The total range of storm bias factors, computed as the ratio of the largest network value divided by the smallest value, is 2.53 (Table 2). The correlation coefficient between radar-estimated and gauge-observed rainfalls is 0.87. The root-mean-square error is 7.9 mm. Removing the bias, simply by multiplying the radar estimates by 0.94, lowers the rmse to 7.7 mm, a fractional standard error of 46%. For a similar experiment with the S-Pol radar conducted in Kansas (Brandes et al. 1999), the FSE was 34%. The larger error in Florida is attributed to smaller storm sizes, shorter lifetimes, higher precipitation gradients, and related sampling issues.

The specific differential phase rainfall estimator for

TABLE 2. Summary results for polarimetric rainfall estimators with Green's axis ratios (Eqs. (3)–(6)) and for empirical axis ratios [Eqs. (7)–(10)]. Rmse is in millimeters.

	Equilibrium axis ratios			
	$\Re(Z_H)$	$\Re(K_{DP})$	$\Re(K_{DP}, Z_{DR})$	$\Re(Z_H, Z_{DR})$
Mean bias factor	0.95	1.17	1.10	0.80
Bias factor range	2.55	2.67	2.43	1.82
Correlation coefficient	0.87	0.86	0.89	0.92
Rmse	7.8	8.2	7.4	8.8
Rmse (bias removed)	7.7	8.1	7.3	6.3
	Empirical axis ratios			
	$\Re(Z_H)$	$\Re(K_{DP})$	$\Re(K_{DP}, Z_{DR})$	$\Re(Z_H, Z_{DR})$
Mean bias factor	0.94	0.97	0.92	0.97
Bias factor range	2.53	2.57	2.38	1.79
Correlation coefficient	0.87	0.87	0.89	0.92
Rmse	7.9	8.0	7.4	6.4
Rmse (bias removed)	7.7	7.8	7.1	6.3

Green's equilibrium axis ratios gives a 17% underestimate of the rainfall. The overall bias factor for the empirical shapes relation gives a small overestimate (~3%). This is a little surprising in view of the discrepancy between the radar and disdrometer estimates of K_{DP} (Table 1). Inspection of Table 3 reveals that among the three events presented in Fig. 2 and summarized in Table 1, the 21 August event has a partic-

ularly large bias factor (1.67), suggesting an unusual DSD or unknown sampling problem for this event. Overall, rainfall estimates for the empirical axis ratio relation increased roughly 20% from those assuming equilibrium axis ratios, a significant shape dependency. Bias factors for individual events vary from a low of 0.65 to a high of 1.67 (Table 3), a range of 2.57 (Table 2). The overall correlation coefficient between gauge

TABLE 3. Summary of polarimetric radar estimates of rainfall for DRGN and KSCN: $\langle G \rangle$ is the avg rainfall amount (mm) at gauges with rainfall, σ_G is the std dev of the gauge amounts, $\Sigma G/\Sigma R$ is the sum of the gauge amounts at gauges with measurable rain divided by the sum of the radar estimates at those gauges. Rainfall estimators are derived from Florida measurements [Eqs. (7)–(10)] and based on the empirical axis ratios [Eq. (2)].

Date	No. gauges	$\langle G \rangle$	σ_G	Bias factors, $\Sigma G/\Sigma R$			
				$\Re(Z_H)$	$\Re(K_{DP})$	$\Re(K_{DP}, Z_{DR})$	$\Re(Z_H, Z_{DR})$
DRGN							
5 Aug	12	22.5	15.2	0.78	0.84	0.95	1.03
6 Aug	12	6.5	3.3	0.62	0.81	0.85	0.79
8 Aug	12	14.1	8.9	0.85	0.81	0.89	1.05
20 Aug	12	14.7	7.0	1.27	1.35	0.92	0.86
21 Aug	12	27.4	5.9	1.44	1.67	1.50	1.27
4 Sep	10	7.4	7.0	1.07	0.94	0.84	0.93
7 Sep	9	12.2	8.2	1.09	1.30	0.94	0.92
17 Sep	10	54.2	10.0	1.15	1.10	0.90	0.96
19 Sep	9	12.6	2.4	0.94	1.00	0.79	0.91
20 Sep	8	10.5	1.1	1.56	1.60	0.91	1.09
21 Sep	10	7.9	6.9	0.90	0.87	0.73	0.96
22 Sep	10	22.1	18.1	0.86	0.79	0.86	0.98
25 Sep	8	5.8	1.9	1.00	0.80	0.64	0.72
KSCN							
5 Aug	25	17.3	12.8	0.63	0.79	0.84	0.85
6 Aug	25	12.3	17.7	0.71	0.75	0.78	0.86
13 Aug	20	10.1	5.2	0.79	0.80	1.10	1.29
1 Sep	17	21.0	21.2	0.84	0.78	0.84	0.97
2 Sep	23	23.3	18.3	0.96	0.94	0.92	0.88
7 Sep	18	10.9	8.0	1.01	1.18	1.01	0.86
17 Sep	21	16.1	21.1	1.06	1.37	1.23	1.08
18 Sep	21	17.4	12.1	1.15	0.98	0.88	1.12
19 Sep	22	13.1	8.5	1.17	1.18	1.02	1.12
21 Sep	21	16.3	16.0	0.95	0.96	0.85	1.01
22 Sep	20	7.7	8.9	0.76	0.65	0.63	0.95
25 Sep	21	31.1	18.8	1.07	1.06	0.96	0.94
Summary	388	16.7	15.7				

Bias Summary PRECIP98

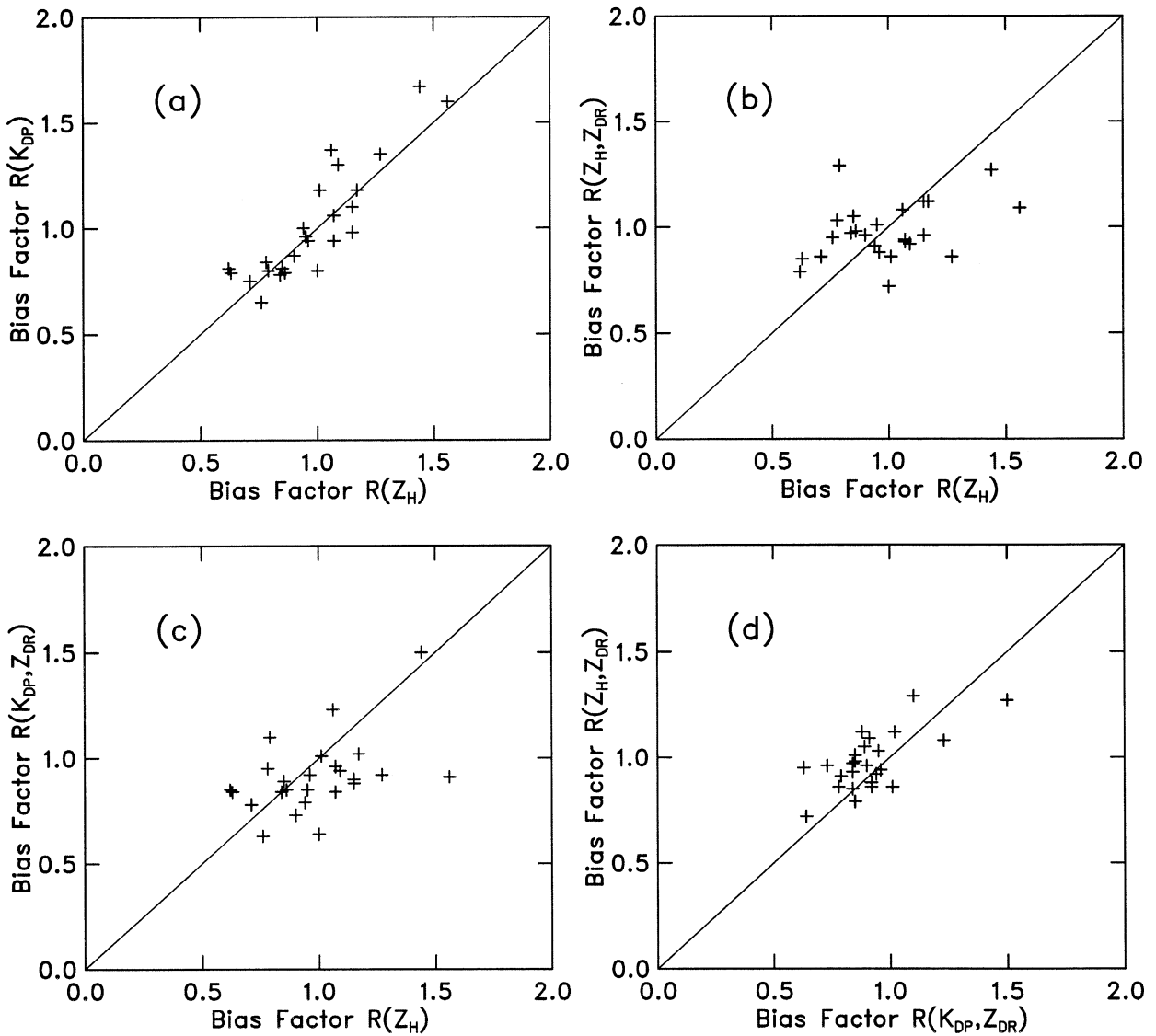


FIG. 3. Plots of bias factors for rainfall estimators derived with empirical axis ratios: [Eqs. (7)–(10)].

and radar amounts is 0.87; the rmse is 8.0 mm; and, if the bias is removed, the rmse is 7.8 mm.

Overall bias factors for the $\mathfrak{R}(K_{DP}, Z_{DR})$ rain-rate estimators are 1.10 and 0.92, respectively. The range in bias factors is somewhat smaller, the correlation coefficient slightly larger, and the rmses are smaller than with either of the single-parameter rainfall estimators. The reflectivity–differential reflectivity relation with equilibrium axis ratios [Eq. (6)] overestimated the rainfall by 25%. Results for the empirical axis ratio relation Eq. (10) gave an overall bias factor of 0.97. Individual storm bias factors vary from 0.72 to 1.29, a range of only 1.79. The correlation coefficient between radar estimates and gauge observations is 0.92. The rmse error

is 6.4 mm which falls to 6.3 mm (a FSE of 38%), if the residual bias is removed.

As found previously (Brandes et al. 2001), our results suggest that performance of radar reflectivity and specific differential phase estimators are equivalent, particularly in terms of the range in bias factors from storm to storm, correlations between rainfall estimates and gauge observations, and the rmse after removing estimator bias. The two-parameter estimators [$\mathfrak{R}(K_{DP}, Z_{DR})$, $\mathfrak{R}(Z_H, Z_{DR})$] have advantages over single-parameter estimators because they partly account for changes in median drop size through the Z_{DR} parameter. This capability reduces the bias factor range and increases the correlation with gauge observations. On average, however,

PRECIP98

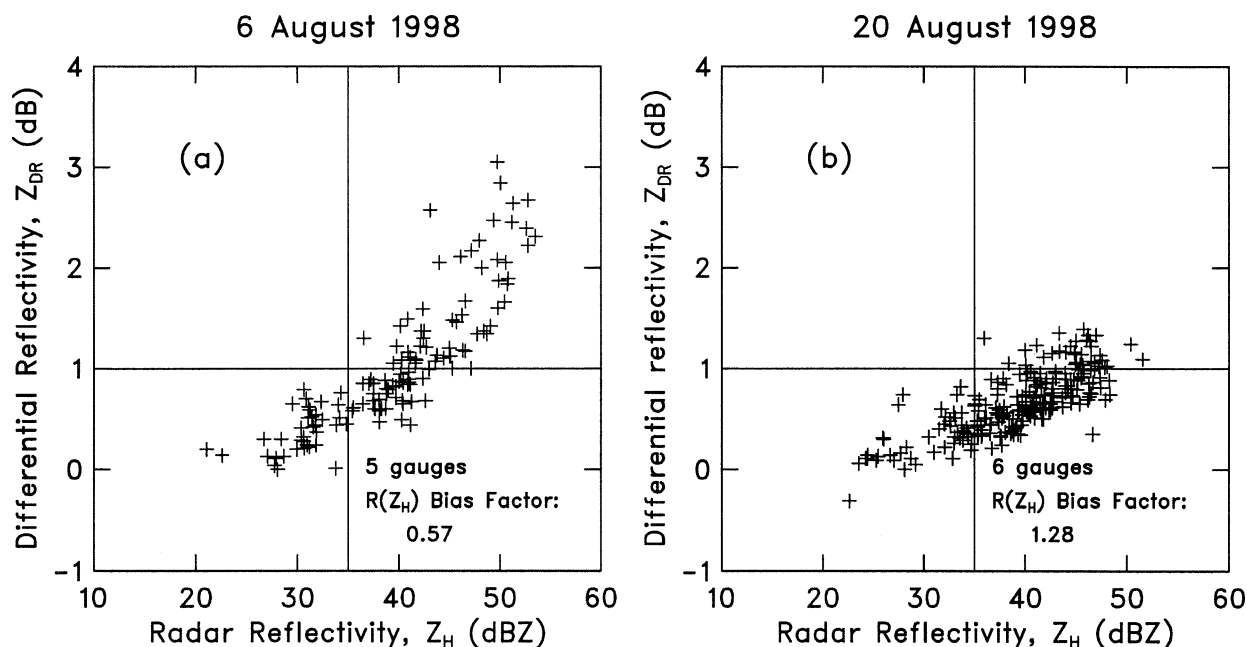


FIG. 4. Radar reflectivity–differential reflectivity distributions for precipitation events occurring on (a) 6 Aug and (b) 20 Aug 1998. The radar reflectivity bias factor at a subset of the gauge sites (those with significant rain) is shown. Only data points with radar reflectivity ≥ 20 dBZ are plotted.

best results in terms of the range in bias factors, correlation coefficients, and the rmse are with $\mathfrak{R}(Z_H, Z_{DR})$ estimators. The high level of performance occurs even though application includes low rain rates where Z_{DR} measurement errors could be important. The reduced performance of the K_{DP} – Z_{DR} combination relative to Z_H – Z_{DR} probably stems from the high error level in Φ_{DP} measurements (especially at low signal levels), the long averaging interval required to compute K_{DP} , and a smaller dependence on differential reflectivity as indicated by the relation exponent.

The impact of the empirical axis ratio relation on the polarimetric estimators was fairly dramatic. Changes in the mean rainfall estimates were on the order of 20%, and overall biases were much reduced. However, impacts on the variation in bias factors from storm to storm, the correlation coefficient between radar-estimated and gauge-observed rainfalls, and the rmse after removing estimator bias were small.

Results for the two gauge networks (Table 3) disclose small differences. Bias factors for $\mathfrak{R}(Z_H)$ and $\mathfrak{R}(K_{DP})$ estimators average about 10% lower in KSCN than in DRGN; rainfall estimates show relative increases over the distance represented by the two networks. $\mathfrak{R}(K_{DP}, Z_{DR})$ and $\mathfrak{R}(Z_H, Z_{DR})$ estimators show bias decreases of $< 3\%$. Zhang et al. (2001b) investigated the possible role of radar sampling effects on $\mathfrak{R}(Z_H)$ and $\mathfrak{R}(Z_H, Z_{DR})$ estimators and show that inhomogeneities within an ever-broadening radar beam could explain their range

response. The K_{DP} -based estimators would behave similarly.

c. Radar evidence of drop-size variation contributions to estimator bias

Although there are storm differences, bias factors for the $\mathfrak{R}(Z_H)$ and $\mathfrak{R}(K_{DP})$ estimators (Table 3) are closely related (Fig. 3a). When there is a sizeable rainfall underestimate with radar reflectivity (indicated by a large bias factor), there is a sizeable underestimate with specific differential phase as well. This correspondence was also found for storms in Colorado and Kansas (Brandes et al. 2001). Agreement is believed due, in large part, to a dependence with both estimators on drop size. A plot of bias factors for $\mathfrak{R}(Z_H)$ and $\mathfrak{R}(Z_H, Z_{DR})$ estimators shows little correlation (Fig. 3b). Reduced agreement in this case is attributed to the capacity of the $\mathfrak{R}(Z_H, Z_{DR})$ estimators to partly accommodate changes in the DSD. Figs. 3c and 3d show the bias correspondence between other pairs of estimators. A positive correlation exists in all cases. The correspondence in Fig. 3d is probably enhanced by the inclusion of Z_{DR} in both estimators. There is no correlation between individual storm bias factors for any of the estimators and the average rainfall amount.

Differential reflectivity is sensitive to the flattening of raindrops and increases with drop size. Hence, variations in Z_{DR} at constant reflectivity are evidence for

PRECIP98

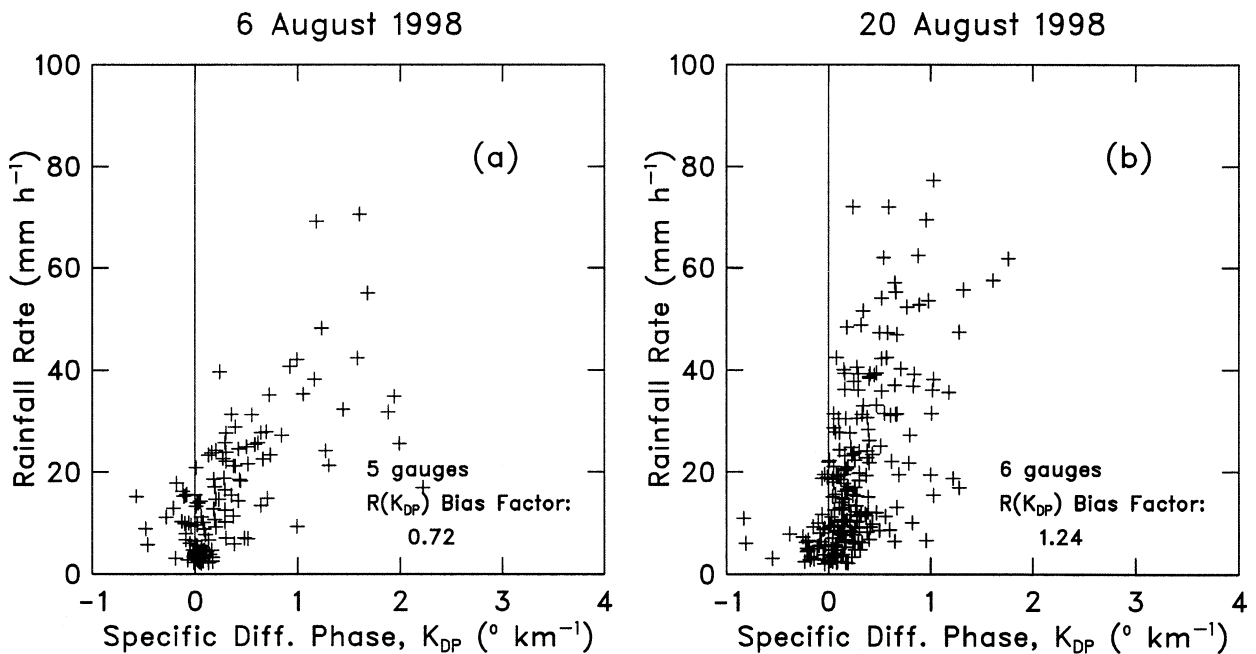


FIG. 5. Radar-derived specific differential phase plotted against gauge-observed rainfall rate for (a) 6 Aug and (b) 20 Aug 1998.

fluctuations in the drop median volume diameter. In Fig. 4, radar reflectivity and differential reflectivity measurements from 6 and 20 August, days with widely varying bias factors with radar reflectivity (and specific differential phase), are plotted. Each data point represents a measurement pair for a particular gauge site and radar scan. Only measurements with radar reflectivity >20 dBZ at gauges with significant rainfall are shown. The bias factor for reflectivity-based rainfall estimates Eq. (7) at the subset of gauges is also given. On 6 August a radar reflectivity factor of 45 dBZ roughly corresponds with a differential reflectivity of about 1.4 dB. On 20 August the same reflectivity associates with a Z_{DR} of ~ 1 dB. Rain rates from Eq. (10) are 51 and 79 mm h^{-1} , respectively. The difference is far more dramatic for reflectivities greater than 45 dBZ. The 6 August event with large Z_{DR} at the higher reflectivity values is dominated by large drops. The reflectivity bias factor (0.57) reflects the tendency to overestimate the rainfall. The smaller drops on 20 August cause a relative rainfall underestimate with reflectivity (a bias factor of 1.28). Clearly, DSD variations have a pronounced effect on rainfall accumulations computed with fixed radar reflectivity estimators.

Figure 5 shows radar-derived specific differential phase plotted against gauge-observed rainfall rate for the events in Fig. 4. The large scatter among data points and large number of negative K_{DP} s at rainfall rates less than 20 mm h^{-1} are readily apparent. On 20 August (the small-drop event) a K_{DP} of $0.5^\circ \text{ km}^{-1}$ associates with an observed rain rate of $\sim 40 \text{ mm h}^{-1}$. On 6 August

(the large-drop event) the same K_{DP} value corresponds to a rain rate of roughly 25 mm h^{-1} . The variation in drop size causes a rainfall overestimate on 6 August and an underestimate on 20 August with Eq. (8). The sensitivity of fixed radar reflectivity and specific differential phase estimators to drop size causes the agreement in bias factors (Fig. 3a).

4. Summary and conclusions

This study of rainfall estimation in a subtropical environment began with a comparison of polarimetric parameters as determined from radar measurements and derived from disdrometer observations. Radar-measured differential reflectivities for three storm events averaged 0.25 dB less than those computed from DSD observations, assuming raindrops with equilibrium axis ratios as given by Green (1975). The departure is much larger than anticipated from calibration procedures but is consistent with several other studies suggesting that oscillating drops in the free atmosphere are more spherical on average than equilibrium shapes. Incorporating empirical (less oblate) drop shapes given by Eq. (2) reduced the difference to 0.06 dB. Radar-estimated specific differential phase had a mean value of $0.15^\circ \text{ km}^{-1}$ as compared with a value of $0.26^\circ \text{ km}^{-1}$ calculated from the disdrometer measurements assuming equilibrium axis ratios. The use of the empirical axis ratios reduced the difference to $0.06^\circ \text{ km}^{-1}$. Hence, the radar-disdrometer comparison was much improved when the drops were assumed to be more spherical.

Rainfall estimators were derived from the disdrometer observations for radar reflectivity, the specific differential propagation phase, the parameter combination of specific differential phase and differential reflectivity, and the combination of reflectivity and differential reflectivity. Estimators were produced for equilibrium and the empirical axis ratios. Radar reflectivity estimators were insensitive to assumed axis ratios. In the mean, the two radar reflectivity estimators gave a small overestimate of the precipitation (about 5%, Table 2). The correlation coefficient between rainfall estimates and gauge observations was relatively high (0.87), the storm-to-storm range in bias factors varied from 2.53 to 2.55, and rmse were 7.8–7.9 mm. After estimator bias was removed, the rmse was 7.7 mm for both estimators.

Polarimetric rainfall estimators [$\mathfrak{R}(K_{DP})$, $\mathfrak{R}(K_{DP}, Z_{DR})$, and $\mathfrak{R}(Z_H, Z_{DR})$] derived with equilibrium axis ratios had significant mean bias factors (1.17, 1.10, and 0.80, respectively). Marked bias improvement occurred for estimators derived from the empirical axis ratio relation (0.97, 0.92, and 0.97). Convergence to a value of 1.0 (slightly less than 1.0 if gauge undercatchments are allowed for) is expected for a consistent set of estimators developed from representative DSDs and a calibrated radar. Convergence in the mean attests to the robustness of the derived axis ratio relation to account for the effective shape of the drops. Although overall agreement among estimators for the experiment is gratifying, large variance remained for individual storms.

Comparison of the single-parameter radar reflectivity and specific differential phase estimators reveals that performance, as measured by the correlation between radar and gauge rainfalls, the range in bias factors, and the rmse after removing residual estimator biases, is similar. There are, however, well-documented situations for which $\mathfrak{R}(K_{DP})$ estimators have distinct advantages over reflectivity; for example, whenever there is a significant hardware calibration error, or the radar beam is partly blocked, or attenuation occurs, or anomalous propagation is present.

Two-parameter estimators gave general improvement over single-parameter relations. The improvement comes from the inclusion of the Z_{DR} measurement to account for changes in drop median volume diameter. For the K_{DP} – Z_{DR} relation based on empirical axis ratios, the overall bias factor was 0.92, the range in bias factors was 2.38, the correlation coefficient between radar and gauge amounts was 0.89, and the rmse (bias removed) was 7.1 mm. Best performance, however, was obtained with an $\mathfrak{R}(Z_H, Z_{DR})$ estimator using the empirical axis ratios. The overall bias factor was 0.97, the range in bias factors was 1.79, the correlation coefficient between radar and gauge amounts was 0.92, and the rmse after removing the estimator bias was 6.3 mm. Reduced performance with the K_{DP} – Z_{DR} parameter pair relative to Z_H – Z_{DR} is attributed to a high error level in the basic Φ_{DP} measurements and the long filtering interval in com-

puting K_{DP} . The larger exponent with the $\mathfrak{R}(Z_H, Z_{DR})$ estimator apparently makes it more responsive to changes in Z_{DR} . This advantage requires that the measurement error be small.

How well our results match other studies is difficult to determine given differences in precipitation climatology, computational procedures, and comparative parameters. A factor-of-2 improvement predicted by simulations and studies with drop-size observations cited in the introduction was not achieved. The reduction in FSE from 46% for radar reflectivity to 38% for the reflectivity–differential reflectivity pair is quite modest. The decrease in the range of bias factors of 29% and the increase in correlation (0.05) are advantages. Yet another benefit is an ability with polarimetric measurements to identify problems with hardware calibration, unusual DSDs, beam blockage, and ground clutter when the various estimators do not agree.

Our results indicate that benefits gained by further fine-tuning of the estimators for shape effects will be small and primarily in mean bias reduction. Correlation coefficients between radar-derived and gauge-observed rainfall accumulations, the range in bias factors from storm to storm, and the rmse after removing residual bias will not change appreciably. Moreover, bias errors on the order of 10% or less can have a multitude of sources. We believe further improvement in rainfall estimation will come from the development of techniques to reduce storm-to-storm and within-storm biases. For $\mathfrak{R}(Z_H)$ estimators this might be accomplished by monitoring the size of the drops with the Z_{DR} parameter and making appropriate adjustments to the coefficient of the Z – R relation. Another possibility is to derive the governing parameters for either exponential or pseudogamma DSDs directly from the measurements and then compute the rain rate (e.g., Seliga et al. 1981; Zhang et al. 2001a).

Acknowledgments. The efforts of several colleagues greatly facilitated this work. Alexander Ryzhkov of the National Severe Storms Laboratory provided the computer code used to derive the specific differential phase from radar measurements and graciously provided comments on our original manuscript. Bradford Fisher of Science Systems and Technology, Inc. assembled the rain gauge data. The disdrometer observations were obtained from Anton Kruger and Witold Krajewski of the University of Iowa. The assistance of National Center for Atmospheric Research staff is also appreciated. Radar operators were Donald G. Ferraro, Alan D. Phinney, Timothy D. Rucker, Michael G. Strong, and Joseph R. Vinson. The flawless performance of S-Pol during PRE-CIP98 is a tribute to Jonathan S. Lutz, the chief radar architect and engineer. Robert A. Rilling and Jean E. Hurst prepared the radar data tapes for analysis, and Benjamin Hendrickson ran the computer programs. This research was supported by funds from the National Sci-

ence Foundation that have been designated for the U.S. Weather Research Program at NCAR.

REFERENCES

- Andsager, K., K. V. Beard, and N. F. Laird, 1999: Laboratory measurements of axis ratios for large drops. *J. Atmos. Sci.*, **56**, 2673–2683.
- Aydin, K., and V. Giridhar, 1992: C-band dual-polarization radar observables in rain. *J. Atmos. Oceanic Technol.*, **9**, 383–390.
- , V. N. Bringi, and L. Liu, 1995: Rain-rate estimation in the presence of hail using S-band specific differential phase and other radar parameters. *J. Appl. Meteor.*, **34**, 404–410.
- Balakrishnan, N., and D. S. Zrnić, 1990: Estimation of rain and hail rates in mixed-phase precipitation. *J. Atmos. Sci.*, **47**, 565–583.
- Beard, K. V., 1984: Oscillating models for predicting raindrop axis and backscattering ratios. *Radio Sci.*, **19**, 67–74.
- , and A. R. Jameson, 1983: Raindrop canting. *J. Atmos. Sci.*, **40**, 448–454.
- , and C. Chuang, 1987: A new model for the equilibrium shape of raindrops. *J. Atmos. Sci.*, **44**, 1509–1524.
- , and R. J. Kubesh, 1991: Laboratory measurements of small raindrop distortion. Part 2: Oscillation frequencies and modes. *J. Atmos. Sci.*, **48**, 2245–2264.
- , D. B. Johnson, and A. R. Jameson, 1983: Collisional forcing of raindrop oscillations. *J. Atmos. Sci.*, **40**, 455–462.
- Brandes, E. A., J. Vivekanandan, and J. W. Wilson, 1999: Comparison of radar reflectivity estimates of rainfall from collocated radars. *J. Atmos. Oceanic Technol.*, **16**, 1264–1272.
- , A. V. Ryzhkov, and D. S. Zrnić, 2001: An evaluation of radar rainfall estimates from specific differential phase. *J. Atmos. Oceanic Technol.*, **18**, 363–375.
- Bringi, V. N., V. Chandrasekar, and R. Xiao, 1998: Raindrop axis ratios and size distributions in Florida rainshafts: An assessment of multiparameter radar algorithms. *IEEE Trans. Geosci. Remote Sens.*, **36**, 703–715.
- Chandrasekar, V., W. A. Cooper, and V. N. Bringi, 1988: Axis ratios and oscillations of raindrops. *J. Atmos. Sci.*, **45**, 1323–1333.
- , V. N. Bringi, N. Balakrishnan, and D. S. Zrnić, 1990: Error structure of multiparameter radar and surface measurements of rainfall. Part III: Specific differential phase. *J. Atmos. Oceanic Technol.*, **7**, 621–629.
- Goddard, J. W. F., and S. M. Cherry, 1984: The ability of dual-polarization radar (copolar linear) to predict rainfall rate and microwave attenuation. *Radio Sci.*, **19**, 201–208.
- , —, and V. N. Bringi, 1982: Comparison of dual-polarized radar measurements of rain with ground-based disdrometer measurements. *J. Appl. Meteor.*, **21**, 252–256.
- , J. Tan, and M. Thurai, 1994: Technique for calibration of meteorological radars using differential phase. *Electron. Lett.*, **30**, 166–167.
- Gorgucci, E., V. Chandrasekar, and G. Scarchilli, 1995: Radar and surface measurement of rainfall during CaPE: 26 July 1991 case study. *J. Appl. Meteor.*, **34**, 1570–1577.
- , G. Scarchilli, and V. Chandrasekar, 1999: Specific differential phase estimation in the presence of nonuniform rainfall medium along the path. *J. Atmos. Oceanic Technol.*, **16**, 1690–1697.
- , —, and —, 2000: Practical aspects of radar rainfall estimation using specific differential propagation phase. *J. Appl. Meteor.*, **39**, 945–955.
- Green, A. W., 1975: An approximation for shapes of large drops. *J. Appl. Meteor.*, **14**, 1578–1583.
- Gunn, R., and G. D. Kinzer, 1949: The terminal velocity of fall for water droplets in stagnant air. *J. Meteor.*, **6**, 243–248.
- Herzogh, P. H., and A. R. Jameson, 1992: Observing precipitation through dual-polarization radar measurements. *Bull. Amer. Meteor. Soc.*, **73**, 1365–1374.
- Ishimari, A., 1991: *Electromagnetic Wave Propagation, Radiation, and Scattering*. Prentice Hall, 637 pp.
- Jameson, A., 1991: A comparison of microwave techniques for measuring rainfall. *J. Appl. Meteor.*, **30**, 32–54.
- Keenan, T. D., L. D. Carey, D. S. Zrnić, and P. T. May, 2001: Sensitivity of 5-cm wavelength polarimetric radar variables to raindrop axial ratio and drop size distribution. *J. Appl. Meteor.*, **40**, 526–545.
- Nešpor, V., W. F. Krajewski, and A. Kruger, 2000: Wind-induced error of raindrop size distribution measurement using a two-dimensional video disdrometer. *J. Atmos. Oceanic Technol.*, **17**, 1483–1492.
- Pruppacher, H. R., and K. V. Beard, 1970: A wind tunnel investigation of the internal circulation and shape of water droplets falling at terminal velocity in air. *Quart. J. Roy. Meteor. Soc.*, **96**, 247–256.
- , and R. L. Pitter, 1971: A semi-empirical determination of the shape of cloud and rain drops. *J. Atmos. Sci.*, **28**, 86–94.
- Ryzhkov, A. V., and D. S. Zrnić, 1994: Precipitation observed in Oklahoma mesoscale convective systems with a polarimetric radar. *J. Appl. Meteor.*, **33**, 455–464.
- , and —, 1995a: Comparison of dual-polarization radar estimators of rain. *J. Atmos. Oceanic Technol.*, **12**, 249–256.
- , and —, 1995b: Precipitation and attenuation measurements at 10-cm wavelength. *J. Appl. Meteor.*, **34**, 2121–2134.
- , and —, 1996: Assessment of rainfall measurement that uses specific differential phase. *J. Appl. Meteor.*, **35**, 2080–2090.
- , and —, 1998: Beamwidth effects on the differential phase measurements of rain. *J. Atmos. Oceanic Technol.*, **15**, 624–634.
- , —, and D. Atlas, 1997: Polarimetrically tuned R(Z) relations and comparison of radar rainfall methods. *J. Appl. Meteor.*, **36**, 340–349.
- Sachidananda, M., and D. S. Zrnić, 1987: Rain rate estimates from differential polarization measurements. *J. Atmos. Oceanic Technol.*, **4**, 588–598.
- Scarchilli, G., E. Gorgucci, V. Chandrasekar, and A. Dobaie, 1996: Self-consistency of polarization diversity measurement of rainfall. *IEEE Trans. Geosci. Remote Sens.*, **34**, 22–26.
- Schönhuber, M., H. E. Urban, J. P. V. Poiaras Baptista, W. L. Randeu, and W. Riedler, 1997: Weather radar versus 2D-video disdrometer data. *Weather Radar Technology for Water Resources Management*, B. Braga Jr. and O. Massambani, Eds., UNESCO Press, 159–171.
- Seliga, T. A., and V. N. Bringi, 1976: Potential use of radar differential reflectivity measurements at orthogonal polarizations for measuring precipitation. *J. Appl. Meteor.*, **15**, 69–76.
- , —, and H. H. Al-Khatib, 1981: A preliminary study of comparative measurements of rainfall rate using the differential reflectivity radar technique and a raingage network. *J. Appl. Meteor.*, **20**, 1362–1368.
- , K. Aydin, and H. Direskeneli, 1986: Disdrometer measurements during an intense rainfall event in central Illinois: Implications for differential reflectivity radar observations. *J. Climate Appl. Meteor.*, **25**, 835–846.
- Sevruk, B., 1996: Adjustment of tipping-bucket precipitation gauge measurements. *Atmos. Res.*, **42**, 237–246.
- Smyth, T. J., T. M. Blackman, and A. J. Illingworth, 1999: Observations of oblate hail using dual polarization radar and implications for hail-detection schemes. *Quart. J. Roy. Meteor. Soc.*, **125**, 993–1016.
- Ulbrich, C. W., and D. Atlas, 1984: Assessment of the contribution of differential polarization to improved rainfall measurements. *Radio Sci.*, **19**, 49–57.
- Vivekanandan, J., D. N. Yates, and E. A. Brandes, 1999: The influence of terrain on rainfall estimates from radar reflectivity and specific propagation phase observations. *J. Atmos. Oceanic Technol.*, **16**, 837–845.
- Zhang, G., J. Vivekanandan, and E. Brandes, 2001a: A method for estimating rain rate and drop size distribution from polarimetric radar measurements. *IEEE Trans. Geosci. Remote Sens.*, **39**, 830–841.
- , —, and —, 2001b: Effects of random inhomogeneity on radar measurements and rain rate estimation. *IEEE Trans. Geosci. Remote Sens.*, **40**, 223–227.
- Zrnić, D. S., and A. Ryzhkov, 1996: Advantages of rain measurements using specific differential phase. *J. Atmos. Oceanic Technol.*, **13**, 454–464.